Ab Initio Structure Evaluation of Aperiodic Structures in the Rare Earth – Ruthenium Systems

by

Alfred Carlsson

Division of Polymer & Materials Chemistry
Lund University

June 2015

Supervisor: **Professor Sven Lidin**
Examiner: **Professor Jan-Olle Malm**

Postal address
P.O. Box 124
SE-221 00 Lund, Sweden
Web address
www.polymat.lth.se

Visiting address
Getingevägen 60

Telephone
+46 46-222 00 00
Telefax
+46 46-222 40 12

Preface

Professor Sven Lidin is gratefully acknowledged for all help provided and for the support in putting this thesis together. A special thanks is dedicated to all the helpful doctoral students and postdocs at the Division of Polymer & Materials Chemistry and to the examiner Professor Jan-Olle Malm for sparking interesting discussions, helpful advices and for accepting the examiner task.

To Hanna Karlsson: Thank you for your positive attitude and all our thought provoking discussions, and of course for sharing your office with me! Best of luck in your future endeavours.

This thesis has opened a whole new world of crystallography to me as well as giving me inspiring and helpful insights and knowledge in the basics and more advanced aspects of crystallography, analysis techniques and inorganic synthesis.

Abstract

Binary alloys comprising of the rare earth metals along with ruthenium, RE-Ru, have been noted to display superconductivity at low temperatures. Furthermore the alloys display interesting magnetic properties such as anomalies in magnetization measurements below the magnetic ordering temperature. In order to understand how some compounds obtain these intrinsic properties it is vital to investigate the crystallography of the compounds. In this thesis the structure, $LaRu_x$, of compounds comprising praseodymium, neodymium or lanthanum in the 35-38 at. % Ruthenium region has been investigated with modern x-ray diffraction techniques. Other compounds, Er_3Ru_2 and $Y_{44}Ru_{25}$, in the 30-40 at. % Ru region has been noted to show evidence of possible superstructure and has also been examined with x-ray diffraction in order to establish the connection between the two related crystal structures and to fully understand the extent and nature of the structures.

The structure of the incommensurately modulated two composite compound Er_3Ru_2 was solved using the current (3+1)d superspace approach from structure data which was collected with x-ray single-crystal diffraction. The structure solution, performed with the charge-flipping algorithm, resulted in the non-centrosymmetric super-space group *X3 (00γ)0* with $a = b =$ 13.893 (4) Å, c = 4.0005 (12) Å q = 1.572 c*.

The possibility for superstructure descriptions for the $Y_{44}Ru_{25}$ and the $LaRu_x$ compounds could also be concluded. The diffraction patterns of both compounds contained satellite reflections, indicating superstructure. Furthermore the $Y_{44}Ru_{25}$ structure could be solved well with two symmetry incompatible lattices further strengthening the possibility of superstructure. Therefore it could be concluded that these compounds most likely can be well described with the superspace description. The task of describing them in higher-dimensions was not completed in this thesis and is considered future work.

Sammanfattning

Binära föreningar bestående av sällsynta jordartsmetallerna och rutenium uppvisar intressanta egenskaper såsom superledande förmåga och intressanta magnetiska egenskaper. För att förstå varför vissa föreningar uppvisar sådana egenskaper är det essentiellt att studera föreningarnas kristallstruktur. I denna rapport undersöks föreningar, i 35-38 at. % Ru regionen, bestående av praseodym, neodymium eller lantan med hjälp av röntgendiffraktionsanalys. Andra faser i 30-40 at. % Ru, specifikt Er_3Ru_2 och $Y_{44}Ru_{25}$, har uppvisat tecken som tyder på att dessa strukturer bättre kan beskrivas i högre dimensioner, s.k. super-rymden. Även dessa föreningar har undersökts med röntgendiffraktionsanalys för att kunna ge en ny beskrivning av dess kristallstruktur.

Strukturen av den inkommensurat modulerade kompositstruktur föreningen Er_3Ru_2 löstes framgångsrikt med hjälp av den rådande (3+1)d formalismen. Strukturlösningen gjordes med hjälp av programmet Jana2006 som använde data genererad från röntgendiffraktometern. Struktur lösningen resulterande i super-rymdgruppen *X3(00γ)0* med cellparametrarna $a = b =$ 13,893 (4) Å, c = 4,0005 (12) Å q = 1,572 c*.

Den högre dimensionella beskrivningen av de två andra föreningarna utfördes inte i detta arbete. Flera indikationer på att dessa föreningar kan beskrivas väl i högre dimensioner kunde dock påvisas. Diffraktionsmönstren för de båda föreningarna visade sig innehålla, förutom huvudreflektioner, satellitreflektioner vilket indikerar en superstruktur. Föreningen bestående av yttrium och rutenium kunde dessutom beskrivas väl av två symmetriinkompatibla gitter vilket är ytterligare en indikation för förekomsten av en superstruktur.

Table of Content

1. Introduction and Aims of the Study

Binary alloys comprising of the rare earth metals along with ruthenium, RE-Ru, have been noted to display superconductivity at low temperatures. Furthermore the alloys display interesting magnetic properties such as anomalies in magnetization measurements below the magnetic ordering temperature[1], [2], [3]. In order to understand these intrinsic properties several studies aiming to assess compound formation, stoichiometry and crystallography of compounds in the RE-Ru system have been performed. One article specifically focused on R-Ru compounds in the 30-40 at.% Ru region [4]. The article reveals that compounds comprising of lanthanum, praseodymium or neodymium around 35-38 at. % Ru shows a complex crystal structure which is believed to be related, possibly through superstructure, to a second structure, $Y_{44}Ru_{25}$, formed in similar stoichiometry in other rare earth-ruthenium systems. Because of its complex structure and large unit cell the authors report that the real crystal structure of this particular structure could not be determined. The complexity of the structure and the large unit cell is a sign that the structure might be modulated or a composite crystal. The related structure, which show similar powder patterns, can also be suspected to be modulated or composite structure due primarily to the reported presence of a substructure and the large unit cell[4], [5]. Additionally another structure in the 30-40 at.% Ru region, Er_3Ru_2, is reported to have Ru atoms arranged incommensurately with the rest of the structure[4].

1.2. Scope and Aim

Compounds comprising praseodymium, neodymium or lanthanum in the 35-38 at. % Ruthenium region will be thoroughly examined with modern x-ray diffraction techniques with the hope of explicitly determining the crystal structure of the compound. The other compounds in the 30-40 at. % Ru region which show evidence of possible superstructure will also be examined with x-ray diffraction in order to establish the connection between the two related crystal structures and to fully understand the extent and nature of the structures. The synthesis was carried out in an arc melting furnace with subsequent annealing in a muffle furnace. Parts of the samples were grinded and analysed with powder diffraction in order to confirm the phases present while the remaining sample was annealed and analysed with single crystal diffraction for the structure determination. The article strives towards answering the questions, are these three structures aperiodic and therefore better described in higher dimensions and are there any similarities between them?

1.3.Limitations

Since the focus is on solving the particular LaRu structure and examine the other two possibly aperiodic structures and because of the time constraint no other compounds or crystal structures in the rare earth ruthenium system will be examined.

2. Theoretical Background

Extensive research has been performed on the RE-Ru systems as can be seen by the numerous phase diagram analyses and crystal structure determination entries in crystallographic

databases. With the exception of europium all other elements in the rare earth series have been found to form binary compounds with ruthenium[4]. These compounds are crystallizing with ten different crystal structure types when including heavy and light element forms but not including the more complex structures of the scandium compounds[4]. So far none of these crystal structures have been resolved from single crystal data with the superspace approach but at least three of the structures show signs of possible aperiodic behaviour.

2.1. Overview of the relevant structures in the binary systems of R-Ru

Since the focus of this study lies in the determination of the $LaRu_x$, $Y_{44}Ru_{25}$ and Er_3Ru_2 structure types only the related and contiguous phases are of relevance.

2.1.1. $LaRu_x$

For binary alloys consisting of La, Pr or Nd and Ru in the interval 35 – 45 at. % Ru, also reported 38 ± 1 at. % Ru, the existence of the phase RRu_x with undefined stoichiometry in equilibrium with the contiguous phases R_7Ru_3 and RRu_2 has been shown[6]. From single crystal diffraction a tetragonal unit cell of a = 11.3 Å and c = 191.3 Å was derived. The crystal structure has not been determined due to the large size of the unit cell but through similarities in powder diffraction patterns it has been hypothesized that the structure is related to $Y_{44}Ru_{25}$[6]. The large unit cell and the similarity to $Y_{44}Ru_{25}$ suggest the possibility of an aperiodic superstructure.

2.1.2. $Y_{44}Ru_{25}$

Eight Yttrium atoms surround each Ruthenium atom in a square antiprism pattern, which builds up the $Y_{44}Ru_{25}$ structure. The structure is reported orthorhombic, space group *Pnna*, with a = 28.08(1) Å, b = 15.195(5) Å, c = 15.195(9) Å and Z = 4. The $Y_{44}Ru_{25}$ crystal structure is observed in systems comprising Y and Sm-Er with Ru[4], [5]. Additionally the structure has been reported as the orthorhombic superspace group Abma(01γ)ss0. The authors theoretically derived this superspace group from the existing three-dimensional description[7].

2.1.3. Er_3Ru_2

Contiguous phase to $Y_{44}Ru_{25}$, the reported Er_3Ru_2-type structure is characterized by trigonal prisms of Er in columns centred by Ru atoms. The structure is reported hexagonal, space group $P6_3/m$, hP10, with a = 7.875(2) Å, c = 3.931(2) Å, Z = 2. An octahedral arrangement of Er atoms filled with Ru atoms with a very short Ru-Ru distance are found along the c-axis[8]. These Ru atoms occupying the channels are reported not to be in correlation to the rest of the structure, signifying the presence of a possible composite superstructure[8].

2.1.4. Sr_7Pt_3, Th_7Fe_3

Contiguous phase to $LaRu_x$, the crystal structure is found in rare earth – ruthenium systems comprising of La – Nd[4]. The Sr_7Pt_3 crystal structure is orthorhombic, space group *Pnma*, with a = 7.929 (1) Å, b = 24.326 (6) Å, c = 7.100 (4) Å, Z = 4. Pt atoms are surrounded by Sr atoms in trigonal prisms along the c axis. Nets of trigonal prisms joined edge wise three by three along the b axis[9]. An exception is the cerium system which crystallizes with the Th_7Fe_3 structure which is likely due to the valence instability of cerium[4].

2.1.5. Mn_5C_2

Contiguous phase to $Y_{44}Ru_{25}$, the Mn_5C_2 type structure is formed in all RE-Ru systems except Ce and Yb. The RE atoms are positioned in the Mn sites and form tricapped trigonal prismatic voids which are occupied by the Ru atom[10].

2.1.6. $MgCu_2$, $MgZn_2$

Contiguous phase to Er_3Ru_2 and $LaRu_x$, binary alloys containing any of the rare earth elements, except the divalent Eu, forms the compound RRu_2 crystallizing with the C14 and C15 Laves phase[10], [4]. $MgZn_2$ has been reported as a low temperature phase on the Ru poor side of the phase diagram while $MgCu_2$ is prevalent at all temperatures[11]. Superconductivity at low temperatures for some of the rare earth-ruthenium compounds crystallizing with the Laves phase are reported[12].

2.2. Three-dimensional crystal structures

A distinctive property of all crystalline materials is long- as well as short-range order in the atomic or molecular dimensions. A macroscopic single crystal can be built up by periodically repeating the basic unit of the crystal in three dimensions[13]. This basic unit is the smallest repeatable unit and is called the unit cell[14]. In the pursuit of categorizing all different kinds of crystal structures it is beneficial to introduce isomeric operations, which can be used to create a congruent motif of the unit cell. If these operations are applied to the whole space and the space remains unchanged after a certain operation the operations is called a symmetry operation[13], [14]. These symmetry operations in combination with the points, axes or planes on which the operations are implemented can be used to classify the structure. The isometric symmetry operations include translation, rotation, inversion, reflection and combinations of these operations. The operations that leaves at least one point unmoved, e.g. rotation and inversion, define the point group of the crystal and in combination with the translational symmetry operations and the lattice system the space group of the crystal can be determined[13], [14].

There are seven lattice systems, which mathematically describe the equivalent positions in the lattice by three vectors and three angles. Note that the equivalent positions in a lattice is a mathematical description of the repeating structure and is not the same as atomic positions in a crystal[13]. The lattice points can be occupied by atoms, ions, molecules or groups of molecules in a real crystal. The simplest regular array, lattice, can always be defined by a unit cell with a lattice point in each corner called a primitive unit cell. However it is convenient to choose a cell that represents the maximum symmetry of the array while still being the smallest repeatable unit[13], [14]. Therefore there are three additional lattice types, additional to the primitive lattice, which describe the centring of the lattice distributed among the lattice systems to give the 14 Bravais lattices. Because of the periodicity, which arises from the translational symmetry of crystals in three dimensions, crystals are space-filling, there are constraints on which symmetry operations are allowed. For example fivefold rotational axes are not allowed in regular three-dimensional crystals, as these cannot be used to stack unit cells without spaces. Combining these restrictions with the point groups and the Bravais lattices all the 230 three-dimensional space groups can be described[13], [14].

2.3.X-Ray Diffraction

An x-ray diffractometer utilizes the diffraction phenomena that occur when matter interacts with x-rays. The basic components are a source of x-rays, a monochromator and a detector. As x-rays, useful wavelengths for crystallography lies between 0.4 and 2.5 Å, hits the ordered lattice of a crystal they are diffracted, scattered. If the waves have a wavelength of the order of the atomic spacing of atoms a phase difference between the scattered waves occurs which can

be used to derive the positions of atoms[14]. The diffraction occurs as x-rays interacts with electrons in the crystal and is scattered by elastic collisions with electrons[14]. The interaction can cause the photons to be deflected, scattered. This scattering can be low energy which is characterized by no loss off energy and is called Thompson scattering, the interaction can also occur with a small loss of energy which is called Compton scattering. Additionally the incident photons can be absorbed by the target atoms, which often needs to be taken in consideration when solving inorganic structures. The scattering of x-rays are increased by the atomic number of the crystal atoms and the atoms scattering effectiveness is called scattering factor[13]. The scattering factor also depends on the wavelength of the x-rays and the angle between a crystal plane and the incident X-rays called the Bragg angle. Actually the x-rays are not scattered by atoms on a single plane but penetrate deep into the crystal and are reflected by many lattice planes. This will result in a number of reflected waves which can interfere constructively or destructively[13], [14]. In order to derive a reasonable intensity from the reflected waves they must interfere constructively which for a specific crystal plane spacing (d_{hkl}), incident angle (θ_{hkl}) and x-ray wavelength (λ) are described by the Bragg equation (equation 1).

$$n\lambda = 2d_{hkl}sin\theta_{hkl} \tag{1}$$

From this law it's evident that a large unit cell in direct space, i.e. a structure with a large d_{hkl}, will generate a dense diffraction pattern, reciprocal space θ_{hkl}, and vice versa. Since the refractive index of x-rays are close to unity x-rays cannot be focused to form a projected image of the crystal lattice[14]. Instead the intensities of the reflected waves are recorded and the effect of a lens is simulated by mathematical calculations. The atomic positions in the lattice can be derived from the phase of the wave, the phase being the fraction of a wave cycle that has passed since the wave was scattered. However only the intensity, which is the square of the amplitude, is recorded and the phase information is lost. The structure factor (F_{hkl}) (equation 2), which is the Fourier transform of the electron density and the resultant of the waves scattered on the *hkl* plane, is proportional to the square of the intensity (equation 3) and is dependent on the scattering factor and the position of the atoms[13]. This Fourier transform is the mathematically simulated lens, which forms an image of the object.

$$F_{hkl} = \sum f_j e^{2\pi(hx_j+ky_j+lz_j)} \tag{2}$$

$$I_{hkl} \propto F_{hkl}^2 \tag{3}$$

Again the phase information is lost due to the quadratic relationship and only the magnitude of the structure factor can be obtained from the recorded intensities. The problem is then to solve the structure from data where only the amplitude and not the phase of the structure factor is known. In order to solve crystal structures, the intensity for each *hkl* reflection along with the Bragg angle are measured. This data is then subject to a set of corrections, e.g. absorption correction and polarisation correction, called data reduction. The square root of these corrected intensity data results in the observed structure factors, F_{obs}, and from the systematic extinctions the Bravais lattice and the translational symmetry can be deduced[13]. To solve the phase problem a set of trial phases for the structure factors are created by a variety of different methods. Used in this project is a variant of a direct method, the charge-flipping method, which differs slightly from traditional direct methods. This method works by assigning phases to the observed amplitude and calculating an electron density by inverse

discrete Fourier transform. The electron density is then modified so that the sign of points with a positive density below a certain value are flipped, new structure factors are calculated and combined with the observed amplitudes and this process are repeated in iterative cycles[15], [16]. Additional methods are the Patterson method, which utilizes the large scattering caused by heavy atoms to derive the position of the heavy atoms, and the traditional direct methods which through mathematical relationships derives the phase of the structure factors from the observed intensities[14]. The mathematical relationships relate the phase and amplitude of the structure factors by utilizing positivity, the electron density function is everywhere positive, and atomicity, the electron density function is composed of discrete atoms, constraints[14]. By least square methods the position and geometry of the atoms are refined with isotropic or anisotropic parameters to account for the thermal motion of the atoms by applying as set of geometric restraints for e.g. atomic distances and atom shape. A calculated set of structure factors is created at this stage. By comparing the calculated and observed structure factors a residual index (R) is obtained which is a measure of how well the structure has been refined. The residual index is calculated as the sum of the difference between the observed and calculated structure factors divided by the sum of the observed structure factors (equation 4).

$$R = \frac{\sum|(|F_o||F_c|)|}{\sum|F_o|} \tag{4}$$

2.4. Higher-Dimensional Crystallography, Super space and Aperiodic Structures

Since the introduction of higher-dimensional crystallography, crystals readily described in higher-dimensions have been shown to be prevalent in compounds comprising almost all elements[7]. The need for a higher-dimension description of a crystal system arises from the distortion of atomic positions from the original atomic positions that are prevalent in numerous crystals. This distortion is periodic but is independent in respect to the periodicity of the average 3d structure. Despite the perturbations aperiodic structures still show long-range order, which is reflected in the diffraction pattern, reciprocal space, as sharp Bragg reflections. Where the Bragg reflections of three dimensional periodic crystals can be indexed by three integers due their inherent translational symmetry, aperiodic crystals cannot due to the loss of translational symmetry from the perturbation of atomic positions[17].

With the accepted superstructure formalism developed by De Wolff, Janssen and Janner an extra dimension that is the modulation vector, denoted q, is needed in order describe and to restore the translational symmetry which is lost due to the perturbation of the atomic positions[18]. The modulation has two basic types, displacive and occupational. The displacive modulation describes positional deviation and occupational modulation describes a distortion of the probability distribution, i.e. partial occupancies of atomic positions can also lead to aperiodic structures [19]. Additionally the modulation wave function can be harmonic and non-harmonic. Harmonic modulation can be described by a truncated Fourier series and the non-harmonic can be described by a crenel function or a combination of occupational and displacive modulations so called saw-tooth functions[19].

The distortion of atomic positions is not limited to one axis, in which case the q-vector needs to be described with integers in two or more directions. Additionally the complexity of the modulation can give rise to even higher-dimensional crystals in which case additional modulation vectors are required. The periodic perturbation is described by the modulation vector, which can be described by a wave function, and when the ratio of the original atomic distance and the wavelength of the perturbing function is a rational number the structure is called a commensurate modulated structure. In the case where the ratio, denoted γ, is an irrational number the structure is called an incommensurate modulated structure[7].

Modulated structures can be recognized by their diffraction pattern. Prominent, strong, reflections originate from the 3d structure and are called the main reflections. These main reflections are accompanied by weaker satellite reflections which lies at equal distance $\pm q$ from the main reflections and originates from the periodic perturbation[17]. The fact that the average 3d structure is prevalent in the diffraction pattern restricts the point group of the structure[18]. These type of structures are classified as superspace groups where the average 3d structure is distinguished from the additional dimensions by denoting them (3+d)D, where d is an integer equal to the number of modulation vectors required in order to describe the structure[18]. This denotation helps separate the superspace groups which are periodic in superspace from the general higher-dimensional space groups[20].

Other aperiodic structures apart from the modulated structures are composite structures and quasicrystals. Particular for quasicrystals is the non-crystallographic rotational symmetry and the complete absence of translational periodicity in three dimensions[18]. Composite crystals are characterized by the coexistence of two interpenetrating subsystems[21]. The reciprocal space will then also be characterized by two interpenetrating subsystems. These subsystems can interact with each other, which can cause both subsystems to become incommensurately modulated. Generally a superspace approach is needed in order to describe all diffraction spots [17], [19]. The diffraction pattern of composite crystal can look similar to that of the modulated structures. Strong main reflections are often accompanied by weaker reflections but these are usually the main reflections of the secondary component. The main reflections of the secondary component can be regarded as the satellite reflections of the first component and vice versa but each substructure, if modulated which can be caused by interactions between the two subsystems, can give rise to additional satellite reflections.

The general solution of aperiodic structures is performed by first solving the average structure using the charge-flipping method or one of the other methods, direct or heavy atom methods, on the main reflections, and then describe the modulation and the satellite reflections. The charge-flipping algorithm performed by SUPERFLIP[15] implemented in JANA2006[22] applies the Fourier transform in arbitrary dimensions and can be used for solving both periodic and aperiodic structures. This is accomplished by describing the change in basic structural parameters along the modulation vector with a periodic modulation function[15], [19], [23]. Refinement full least square method can then be performed in JANA2006.

3. Experimental Methods

3.1. Synthesis

3.1.1. Arc melting

The high temperatures necessary for melting of ruthenium is easily reached with an arc melting furnace. The synthesis of all the specimen was performed in an Edmund Bühler MAM1 arc melting furnace with a water cooled copper hearth and a tungsten electrode. After cold pressing of the sample pellets in the glove box, around 60 MPa of pressure, the pellet was transferred to the furnace in an air tight container and put in one of the indentations in the copper heart temporarily exposing the pellet to air. The furnace chamber was then evacuated and purged with high purity argon three times and at last filled to 0.5 atm of argon. The samples was melted and re-melted several times to assure compositional homogeneity with varying nonspecific current adjusted to melt the sample but also considering the vapour pressure of the reactants. Afterwards the chamber was opened to the atmosphere, the sample removed and put in a silica tube which was then evacuated, sealed with an oxy-hydrogen burner and annealed in a muffle furnace.

3.1.2. Degassing of ruthenium

The rare earth metals high affinity for oxygen demands a very pure ruthenium powder in order to avoid unnecessary oxide formation. The general method as described in literature was to pour the ABCR 99.99% pure 200 mesh ruthenium powder in a silica tube connected to a vacuum line. The powder would then be degassed in a pipe furnace at 800 ºC for 5h on dynamic vacuum. Unfortunately because of lack of specialized equipment for the available silica tube dimensions another method of degassing ruthenium was used. By melting the Ruthenium powder in the arc furnace, shots with an unblemished chrome metallic finish were procured indicating that the reducing effect of the arc furnace is sufficient. These shots were then used for the synthesis with the various rare earth metal pellets.

3.1.3. Glove box

All rare earth metals are stored, weighed and pressed in an argon filled glove box. Air sensitive samples are opened and stored in the box. Crystal picking and mounting of some samples, were only needed for the Lanthanum compounds, were performed in the glove box.

3.1.4. Starting materials

Table 3.1. Chemicals and materials used in the synthesis.

Chemical	CAS #	Supplier	Article #	Purity
Er	7440-52-0	ABCR	Powder	99.9%
La	7440-91-0	Chempur	Pieces	99.9%
		Alfa Aesar	Pieces	99.9%
Y	7440-65-5	Strem	Powder	99.9%
Ru	7440-18-8	ABCR	Powder	99.9%
Quartz glass				

3.1.5 Sample preparation

A total of 16 syntheses were performed on the rare earth ruthenium systems, the data and details including stoichiometrics of all samples are found in appendix a. Crystals that resulted in good diffraction patterns and subsequently were used for the solution of the structures were found in samples $LaRu_x$ 3.3 and $Y_{44}Ru_{25}$ 1.0.

The $LaRu_x$ 3.3 sample was prepared by synthesis of weighted La pieces (99.9%, Chempur) with degassed Ru (99.9%, ABCR) shots in the arc furnace. The sample was homogenised by melting at least 8 times, the stoichiometry was aimed at 39 at.% Ru and weighing after synthesis, assuming loss of only La due to vaporisation, revealed a stoichiometry of 38.8 at.% Ru. The sample was sealed in evacuated fused-silica ampoules and annealed in a muffle furnace for 10 days at 770ºC.

The $Y_{44}Ru_{25}$ 1.0 sample was prepared by synthesis of weighted, pressed Y pellets (99.9%, Strem) with degassed Ru (99.9%, ABCR) shots in the arc furnace. The sample was homogenised by melting at least 6 times, the stoichiometry was aimed at 36.2 at.% Ru and weighing after synthesis, assuming loss of only Y due to vaporisation, revealed a stoichiometry of about 38 at.% Ru. The sample was sealed in evacuated fused-silica ampoules and annealed in a muffle furnace for 12 days at 770ºC.

Several attempts were made to synthesize the Er_3Ru_2 phase in order to obtain better Er_3Ru_2 crystals. Several attempts were also made to obtain better $Y_{44}Ru_{25}$ crystals but to no avail. All samples of $Y_{44}Ru_{25}$ and Er_3Ru_2 phases after the initial $Y_{44}Ru_{25}$ synthesis were characterized by low crystallinity and existence of gas bubbles in the samples.

3.2. X-ray diffraction

3.2.1. Powder X-ray diffraction

After synthesis a small part of the lightly crushed samples were analysed with powder x-ray diffraction. By comparing experimental powder patterns with documented patterns in crystallographic databases, mainly Pearsons Crystallographic database, in the program WinXPOW phase identification of the samples were possible. The lightly crushed sample was ground to a fine powder and was put on a piece of Magic tape which was then folded and put in the sample holder. The diffractometer was a STOE Stadi Mp with vertical arrangement equipped with an MYTHEN 1k detector. The x-ray source was copper, $K\alpha_1$ λ = 1.5418 Å, with a germanium monochromator. The apparatus was set to transmission $2\theta/\omega$ scan mode in the program suite WinXPow[24] which was also used for data analysis. Si was used as standard for the zero point calibration.

3.2.2. Single crystal X-ray diffraction

Samples were lightly crushed, larger pieces removed and the residual crystals were brought under microscope. Crystals with metallic lustre and clean facets' were glued on silica glass fibres with two component glue. Some of the crystals were particularly prone to oxidation and required a different mounting method in order to get a reasonably good diffraction pattern, this were only needed for the lanthanum compound crystals. These readily oxidizing crystals were instead mounted on crystal mounting loops which were covered in paratone oil. The single crystal intensity data collections were performed on an Oxford Diffraction XCaliburE diffractometer at room temperature. The apparatus was equipped with an EOS CCD detector and the x-ray source is generating Enhance Mo $K\alpha_1$ λ = 0.7107 Å radiation. The alignment of

the crystals was performed with the help of the built in video microscope linked to a LCD monitor on the apparatus. Data collection, reduction and integration were performed with the diffractometer control program CrysAlisPro[25]. Numerical absorption correction, polarization correction and the Lorentz correction was applied in the data reduction. All structures were solved using the charge-flipping algorithm with SUPERFLIP[15] and the subsequent refinement was performed in JANA2006[22]. Atom models were created and visualized in the computer program Diamond[26]

4. Results and Discussion

4.1. Er_3Ru_2

Several attempts at synthesising the Er_3Ru_2 crystal structure with Er and Ru were made but all were unsuccessful in procuring sufficiently crystalline samples. The variable, or variables, that caused the Er samples not to crystalize properly has not been eluded but it might be coupled to the same problem that was encountered with the Y-Ru samples. The reason the samples would not crystalize properly could be due to the general state of the arc furnace. This could be, but has not been, tested by thoroughly cleaning the furnace and grind away the accumulations on the electrode.

Some Er_3Ru_2 crystals were obtained from the Er samples but the resulting diffraction patterns were not of sufficient quality and contained lots of unwanted reflections that could not be indexed. Eventually, after running many crystals through the x-ray diffractometer, an Y_3Ru_2 crystal was found in the $Y_{44}Ru_{25}$ 1.0 sample resulting in good diffraction patterns. The diffraction patterns, which are hexagonal R-centred in four-dimensions, indicates a basic cell with cell parameters $a = b = 13.893$ (4) Å, $c = 4.0005$ (12) Å with a total of 742 reflection and an UB fit of 67.25%. Evident from the diffraction patterns are the existence of a superstructure which could not be detected in diffraction patterns from earlier crystals. Strong reflections are accompanied by weaker reflections as can be seen in the *h0l* reflections (Figure 1a)).

Figure 1. a) Layered image, averaged with 2mm symmetry, of the *h0l* reflections showing the strong main reflections of component 1 and the weaker main reflections of component 2. b)

Layered image, averaged with trigonal symmetry, of the *hl14* reflections showing a hexagonal diffraction pattern.

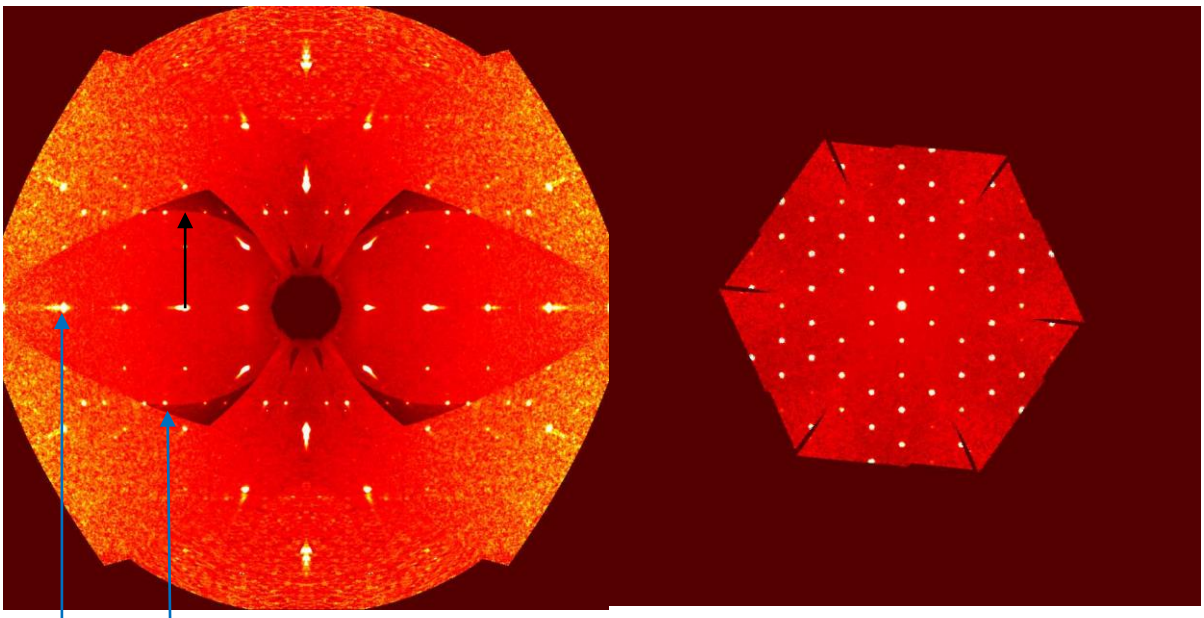

The diffraction pattern indicates a composite superstructure with two subsystems which are parallel, albeit incommensurable, in the c direction. The reflections from the two subsystems can be regarded as the satellites to each other and if the strong main reflections from subunit 1 are regarded as the main of the superstructure the weaker satellite reflections can be indexed by one modulation wave vector q, drawn as a black arrow in Figure 1a), along the c* direction, q = γc*, where γ is approximately equal to 1.572. This vector was defined along with the following four-dimensional rhombohedral extinction conditions in CrysAlisPro before the reduction was executed (equation 5).

$$hklm\colon\ -h+k+m=3n \tag{5}$$

These conditions means that an atom described by the phase ν of modulation function in the position xyz will also be found in the position x + 1/3, y + 2/3, z with phase νπ/3.

Another way of indexing, which would result in classical three dimensional R centring, would be to switch the position of the c*and the q-vector. This would result in the classical R centred extinction condition:

$$hklm\colon\ -h+k+l=3n \tag{6}$$

The first indexation was chosen since it uses the strongest reflections as the base structure.

The presence of a twin in the structure could be detected in the diffraction pattern and need to be corrected for. The twin was oriented along the c-axis rotated 180º in relation to the other component. The twinning matrices are:

$$\begin{pmatrix} -1 & 0 & 0 \\ 0 & -1 & 0 \\ 0 & 0 & 1 \end{pmatrix}$$

The data was loaded in Jana2006 for structural solution and subsequent refinement which resulted in five atomic positions in the non-centrosymmetric four-dimensional unit. The reflections from the two subsystems are defined by the two transformation matrices W^1 and W^2:

$$W^1 = \begin{pmatrix} 1 & 0 & 0 & 0 \\ 0 & 1 & 0 & 0 \\ 0 & 0 & 1 & 0 \\ 0 & 0 & 0 & 1 \end{pmatrix} \; and \; W^2 = \begin{pmatrix} 1 & 0 & 0 & 0 \\ 0 & 1 & 0 & 0 \\ 0 & 0 & 0 & 1 \\ 0 & 0 & 1 & 0 \end{pmatrix}$$

The first subsystem comprises of Ru1 at (2/3, 0, 2.44696), Ru2 at (-2/3, 0 – 0.244696), Y1 at (0.559234, -0.173222, -0.245914) and Y2 at (-0.559234, 0.173222, 0.245914) and the second subsystem is built up exclusively of Ru3 atoms in position (0, 0, 0).

From displacement x4-t plots the displacement of the atoms can be visualized (Figure 2). It's evident that atoms Y1 and Y2 show displacement in all directions, whereas atoms Ru1 and Ru2 only in x-, y-directions and Ru3 only in the z direction.

Figure 2. Modulation functions of the atoms describing the positional displacement of the atoms in x-, y-, z-directions as a function of the incommensurate direction x4. a) dx as a function of x4, b) dy as a function of x4, c) dz as a function of x4.

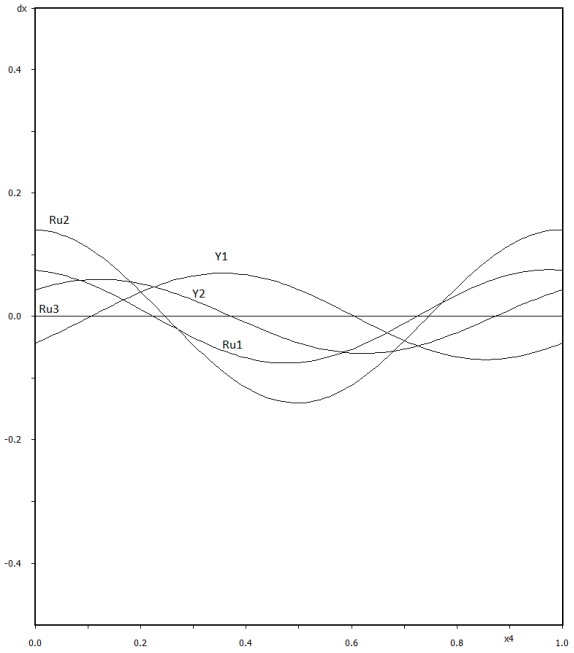

a)

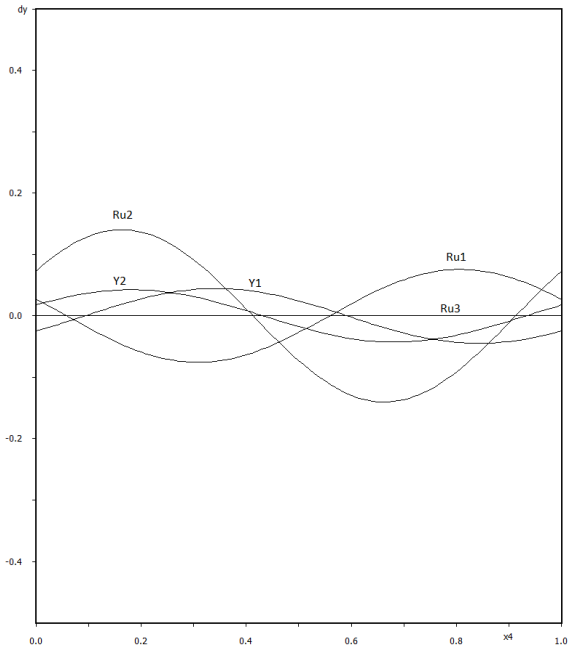

b)

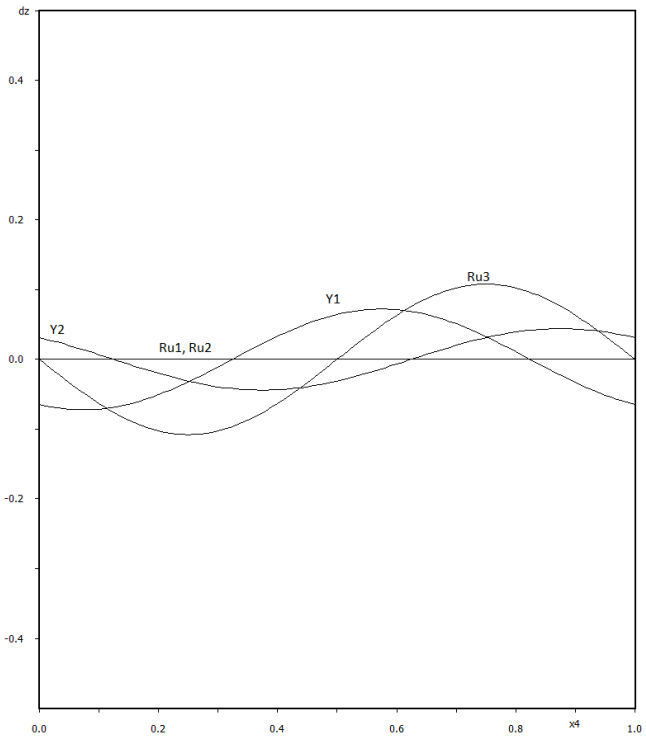

c)

This displacement of atoms, in the a-, b-direction can also be visualized from the three-dimensional atom model viewed along the c- direction (Figure 3).

Figure 3. Two-dimensional projection of the three-dimensional model of the four-dimensional superstructure viewed along the c-direction.

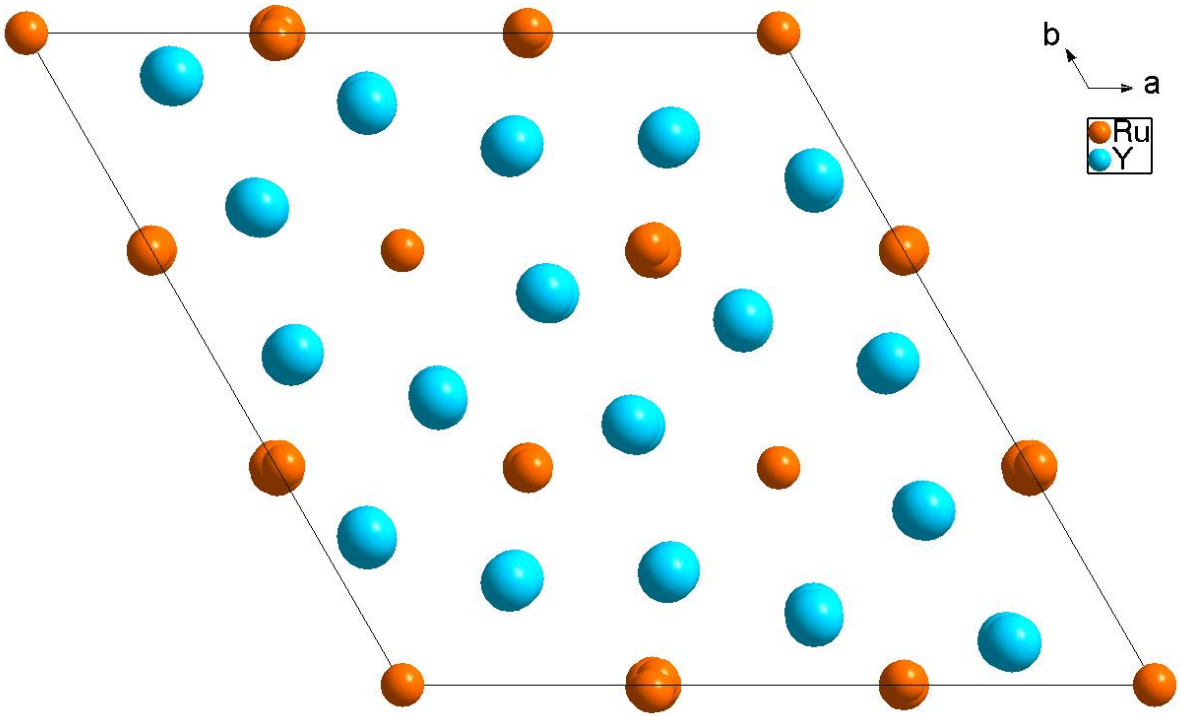

Here we can see how the Y1, Y2, Ru1 and Ru2 atom positions are displaced on the a-b planes along the c-direction.

It's the interactions between the two subsystems that causes the displacements. However the displacement of atoms in the a-b plane arises from the incommensurate displacement modulation in the c-direction, visualized in Figure 4, of the Ru3 atoms which, by symmetry, forces displacement of surrounding atoms in the a-b plane. Hence only the single q-vector in the c*-direction is required in order to fully restore the translational symmetry of the crystal.

Figure 4. Figure showing the incommensurate relationship along the c axis between the two subsystems.

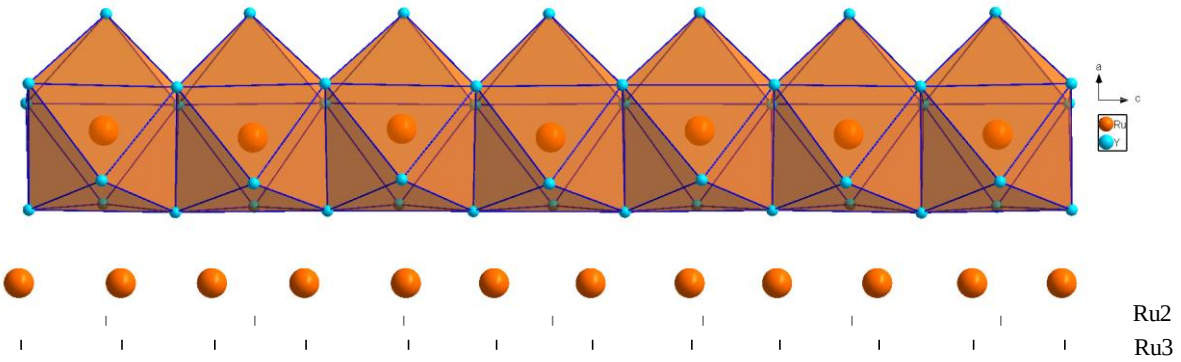

This incommensurate modulation can also be visualized in the plot of the atomic distance between Ru3 and surrounding atoms as a function of the incommensurate parameter *t* (Figure 5).

Figure 5. Atomic distance between Ru3 and surrounding atoms as a function of the incommensurate parameter (*t*). Multiple occurrence of the same atom refer to different atoms related by symmetry.

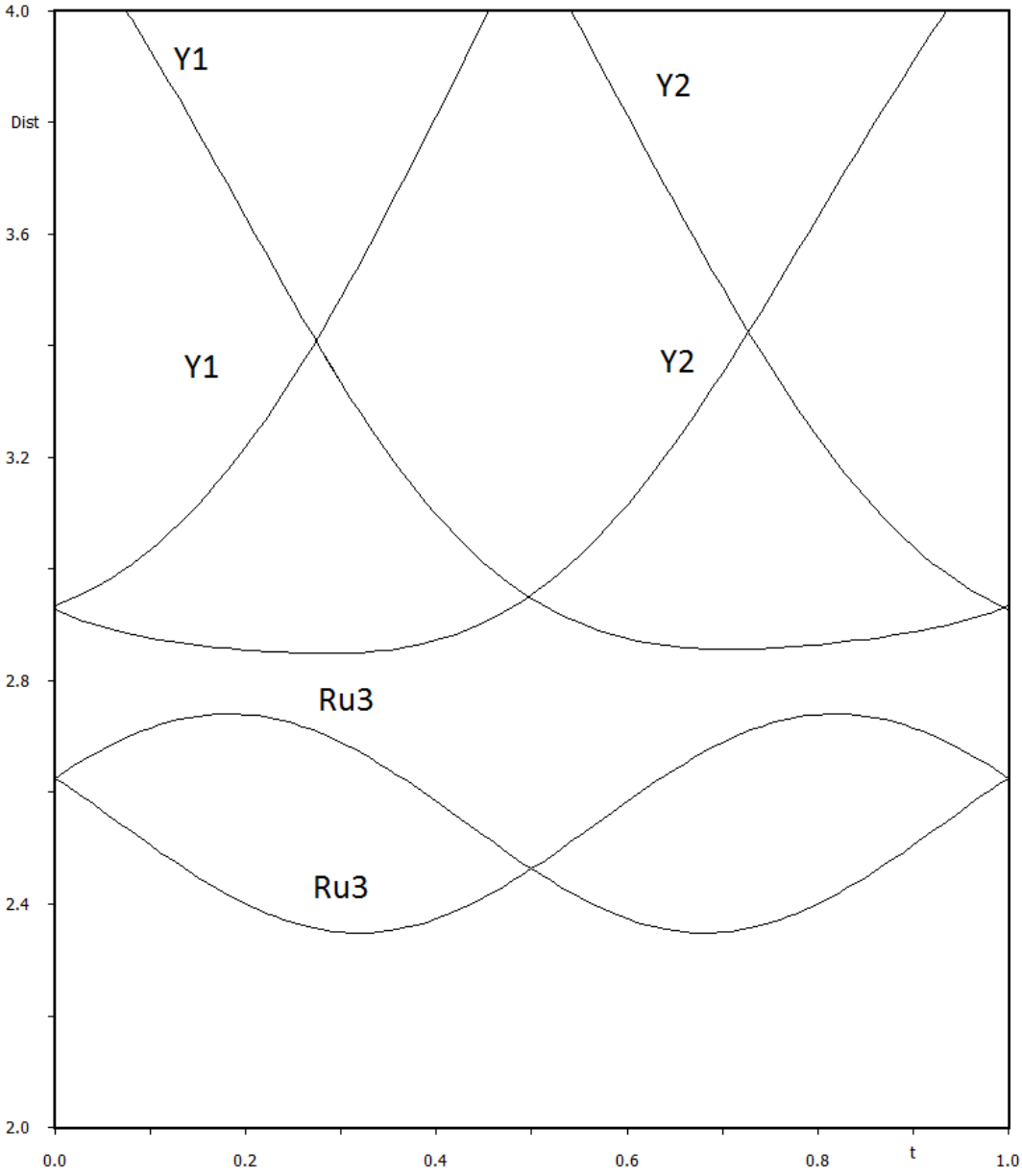

In Figure 5 we see that equivalent Ru3 positions does not have equal distance to equivalent surroundings, the distance to equivalent Y atomic positions go towards infinity as we move along the incommensurate direction. A helpful analogy would be to consider an infinite row of seats with big boned occupants that spill over to adjacent seats. The first occupant will be seated in the first seat but the adjacent occupant will have to move a little further to the side of the respective seat and so on. If the first occupant are considered to belong to the first seat, the second occupant to the second seat and so on it's evident that the occupants will move further

and further away from its equivalent seat as we move along the row. It's this incommensurate modulation that causes the aperiodicity of the structure which demands an additional dimension, modulation vector, in order to restore the translational symmetry of the structure.

For the refinement of the structure several parameters and corrections were introduced. The Y1 atoms were fixed in the x4-direction with the fixed command zcos1[Y1] so as not the whole structure would translate in the x4-direction as the refinement progressed. The model was refined with harmonic atomic displacement parameter, ADP.

Attempts were made to force centrosymmetry on the structure by assigning the following restrictions and equations. The Ru1, Ru2 and Y1, Y2 were restricted so that the ADP of Ru1 is identical to that of Ru2 and Y2 is identical to Y1 respectively. Furthermore the following equations were applied in the refinement commands:

$$x[Ru2] = -x[Ru1]$$

$$y[Ru2] = -y[Ru1]$$

$$z[Ru2] = -z[Ru1]$$

$$x[Y2] = -x[Y1]$$

$$y[Y2] = -y[Y1]$$

$$z[Y2] = -z[Y1]$$

The attempt to force centrosymmetry resulted in a worse description of the structure and the in the final refinement these commands were disabled and the centrosymmetric solution discarded. The structure solution, performed by Superflip, resulted in the non-centrosymmetric super-space group *X3 (00γ)0*. The refinement converged with a goodness of fit, GOF, of 1.04 and the following results:

Table 4.1.1. Refinement results for Y3Ru2.

Component	R_{obs}	wR_{obs}	n_{obs}/n_{all}
Main reflections	2.86 %	3.05 %	625/736
Composite part 1	2.68 %	2.78 %	403/477
Composite part 2	4.64 %	4.27 %	138/161
Common part	2.51 %	3.44 %	84/98

A complete list of crystallographic and technical data for the structure refinement can be found in appendix b.

4.2. $Y_{44}Ru_{25}$

Fairly good diffraction patterns could be obtained from an $Y_{44}Ru_{25}$. Several syntheses were performed to obtain a good $Y_{44}Ru_{25}$ crystal but as in the case of Er_3Ru_2 this was proven a difficult task. The best crystal was found in the first synthesis, $Y_{44}Ru_{25}$ 1.0. The extinction conditions of the main reflections agree with a primitive unit cell. Additionally the presence of a twin rotated around the c-axis can be noted with the following twin matrix:

$$\begin{pmatrix} -1 & 0 & 0 \\ 0 & 1 & 0 \\ 0 & 0 & 1 \end{pmatrix}$$

It's indicated from the satellites in the diffraction pattern that the structure could very well be modulated, either purely modulated or modulated composite (Figure 6). The full higher-dimensional structure solution is not performed in this report but suggestions towards the possible nature of the superstructure are made.

Figure 6. Layered image of the *2kl* reflections, averaged with tetragonal symmetry, showing the main and satellite reflections.

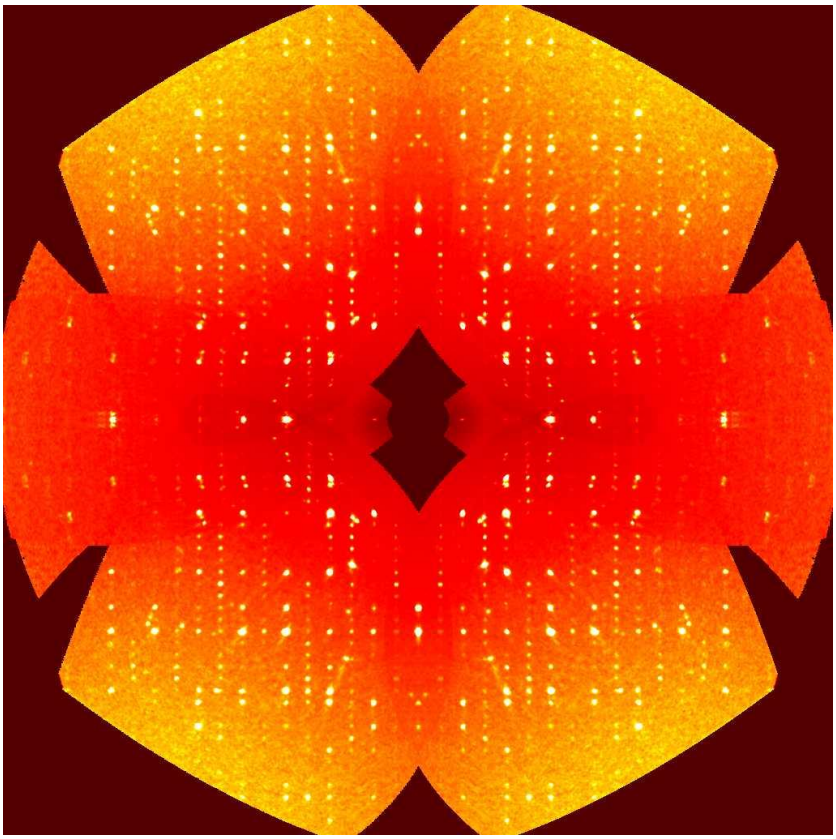

Two structure solutions are presented for the $Y_{44}Ru_{25}$ phase, one is orthorhombic and the other tetragonal.

The orthorhombic solution has been reported earlier by other authors and the solution resulted in the space group *Pnna* with a = 28.08(1) Å, b = 15.195(5) Å, c = 15.195(9) Å and Z = 4. The

structure can be built up solely by ruthenium atoms surrounded by eight yttrium atoms in square antiprism pattern.

The other solution, obtained by the charge-flipping algorithm performed on the diffraction pattern from the $Y_{44}Ru_{25}$ crystal procured from the $Y_{44}Ru_{25}$ 1.0 sample resulted in the space group *P4/n*. The dimensions of the unit cell were a = 15.2584 (Å), b = 15.2584 (Å), c = 28.033 (Å). The refinement, performed with harmonic ADP, resulted in 47 atomic positions which can be found in appendix B. The refinement ended with R_{obs} = 8.49 % over 1426 observed reflections.

The structure can be described with some of the ruthenium atoms surrounded by eight yttrium atoms in the form of square antiprism which forms columns of face sharing antiprisms along the c-direction. The rest of the ruthenium atoms are surrounded by four yttrium atoms in the form of tetrahedron which share edges along the c-direction and form columns that surround the square anti prism columns (Figure 7, 8).

Figure 7. The unit cell of the *P4/n* structure solution of $LaRu_x$ observed along the c-direction with tetrahedrons and square antiprism forming column along the c-direction.

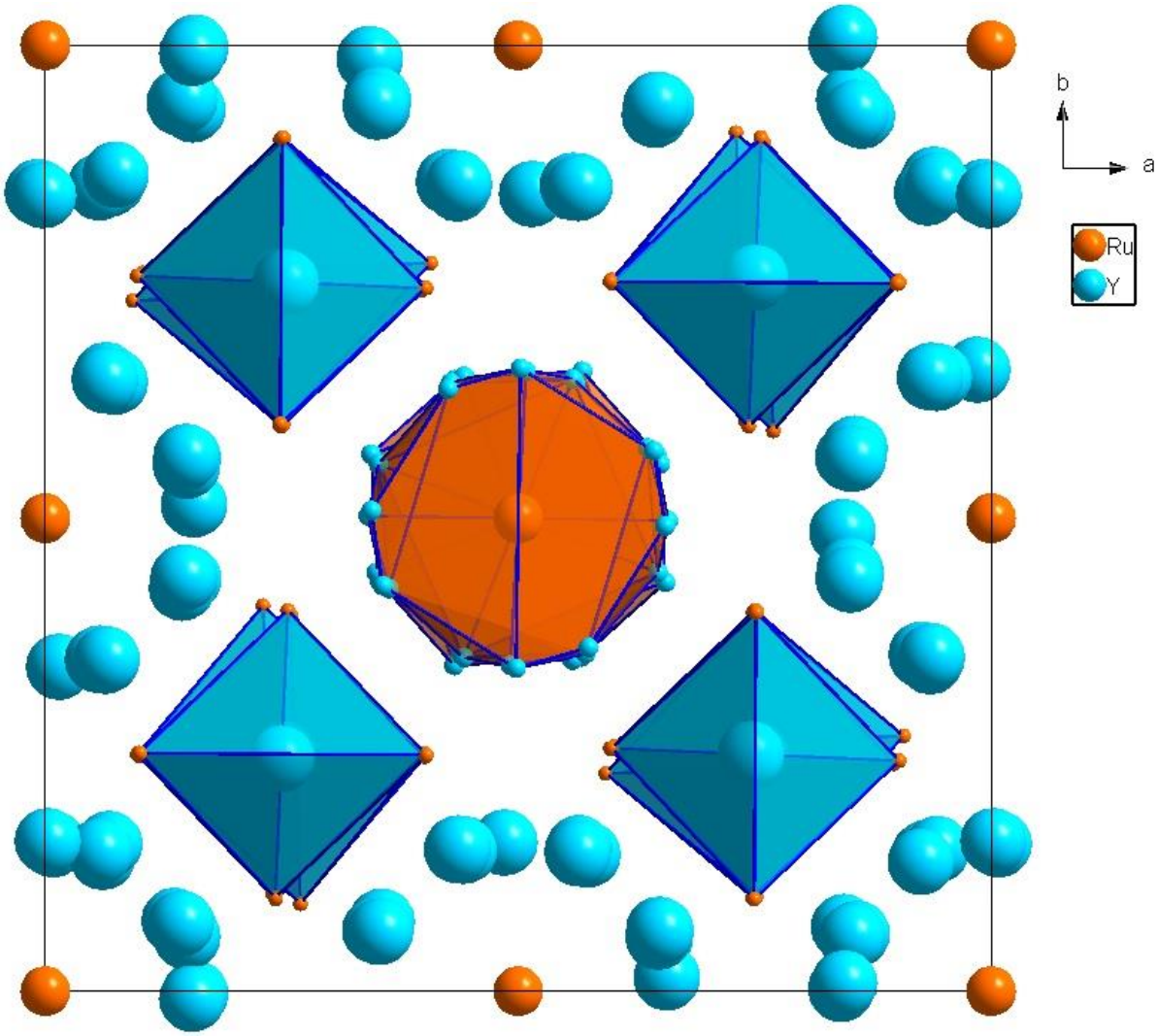

Figure 8. A cut out section of the *P4/n* structure showing how the square antiprism and tetrahedron form their respective columns along the c-direction.

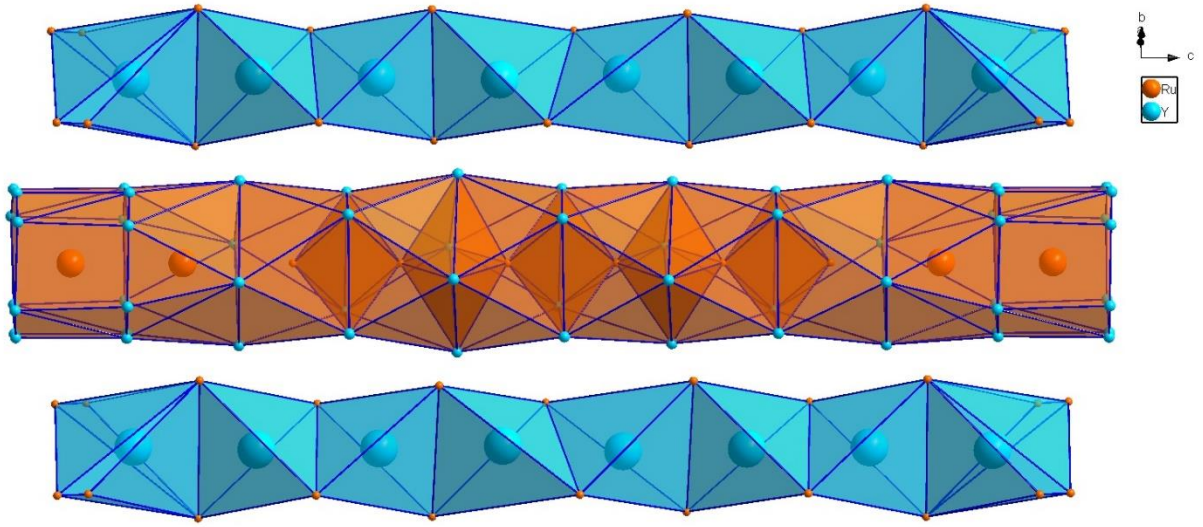

Although the geometry of the atomic correlations, the polyhedrons, are the same it should be noted that the orthorhombic, *Pnna*, and the tetragonal, *P4/n*, lattices are symmetry incompatible. The orthorhombic solution, Laue group mmm, has two-fold symmetry around all axes with reflection perpendicular to them. The Laue group of the tetragonal solution is 4/m, which means that it has four-fold symmetry around the c-axis and reflection perpendicular to the c-axis, hence the tetragonal model lacks orthogonal operations and the solutions are symmetry incompatible. Again the positional perturbation caused by the incommensurability in incommensurate composite structures can lead to more than one equally good structure solution of the three-dimensional lattice. The fact that we can describe the structure with both an orthorhombic and tetragonal lattice is an indication that the structure is aperiodic and can be described well in higher-dimensions.

The higher-dimensional description has proven to be difficult and time consuming and will not be performed in this thesis. The structure has been reported as the orthorhombic superspace group Abma(01γ)ss0 but from the tetragonal solution in this report it's likely that the superspace structure solution will result in a tetragonal unit cell.

4.3.$LaRu_x$

Noisy, but sufficient for structure evaluation, diffraction patterns were generated from a $LaRu_x$ crystal obtained from the $LaRu_x$ 3.3 sample. The systematic extinction conditions of the main reflection agree with a primitive unit cell. In Figure 9 a) the layered *h0l* reflections show the main reflections, intersected by the overlaid grid, and some noise reflections, not on the grid, possibly generated from unwanted crystalline matter adhered to the facets of the crystal.

Figure 9.) Layered image of the *h0l* reflections showing the strong main reflections and additional noise reflections that cannot be indexed by the grid. b) Layered image of the *0kl* reflections showing the main as well as the satellite reflections.

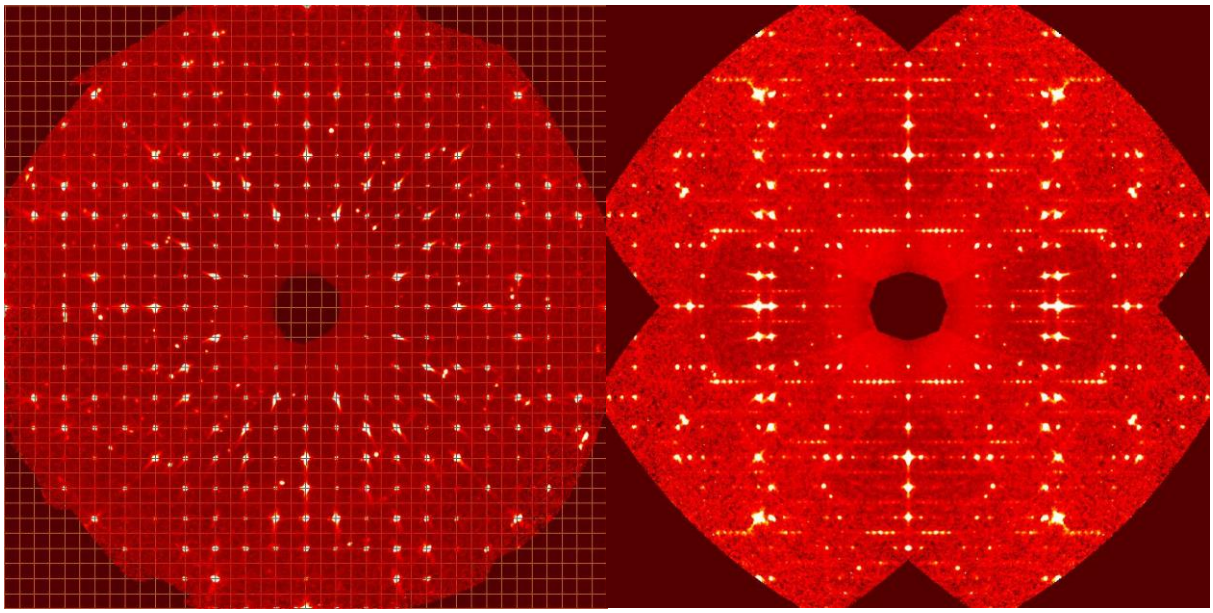

a) b)

The data went through reduction and was then loaded in Jana2006 for the structure solution and refinement. The structure solution, performed with the charge-flipping algorithm (Superflip), resulted in three on par possible Bravais lattice solutions. The best solutions were the primitive and I-centred orthorhombic and primitive tetragonal lattices.

The orthorhombic solution was refined using the $C222_1$ space group and the cell parameters a = 16.0154(4) (Å), b = 16.0154(4) (Å), c = 35.5542(9) (Å). The refinement ended with R_{obs} = 11.79 % over 5492 observed reflections. The refinement was performed with harmonic ADP. The structure is described with 45 atomic positions, these positions can be found in appendix B along with complete list of crystallographic and technical data for the structure refinement.

Some ruthenium atoms are surrounded by eight lanthanum atoms in the form of square antiprism which forms columns of face sharing antiprisms along the c-direction. The rest of the ruthenium atoms are surrounded by four lanthanum atoms in the form of tetrahedron which share edges along the c-direction and form columns situated at the centre of four square anti prism columns (Figure 10, 11). The primitive solution is described in the same way as the I-centred and was also refined with harmonic ADP. The refinement ended with R_{obs} = 14.96.

Figure 10. The unit cell of the *C222₁* structure solution of $LaRu_x$ observed along the c-direction with tetrahedrons and square antiprism.

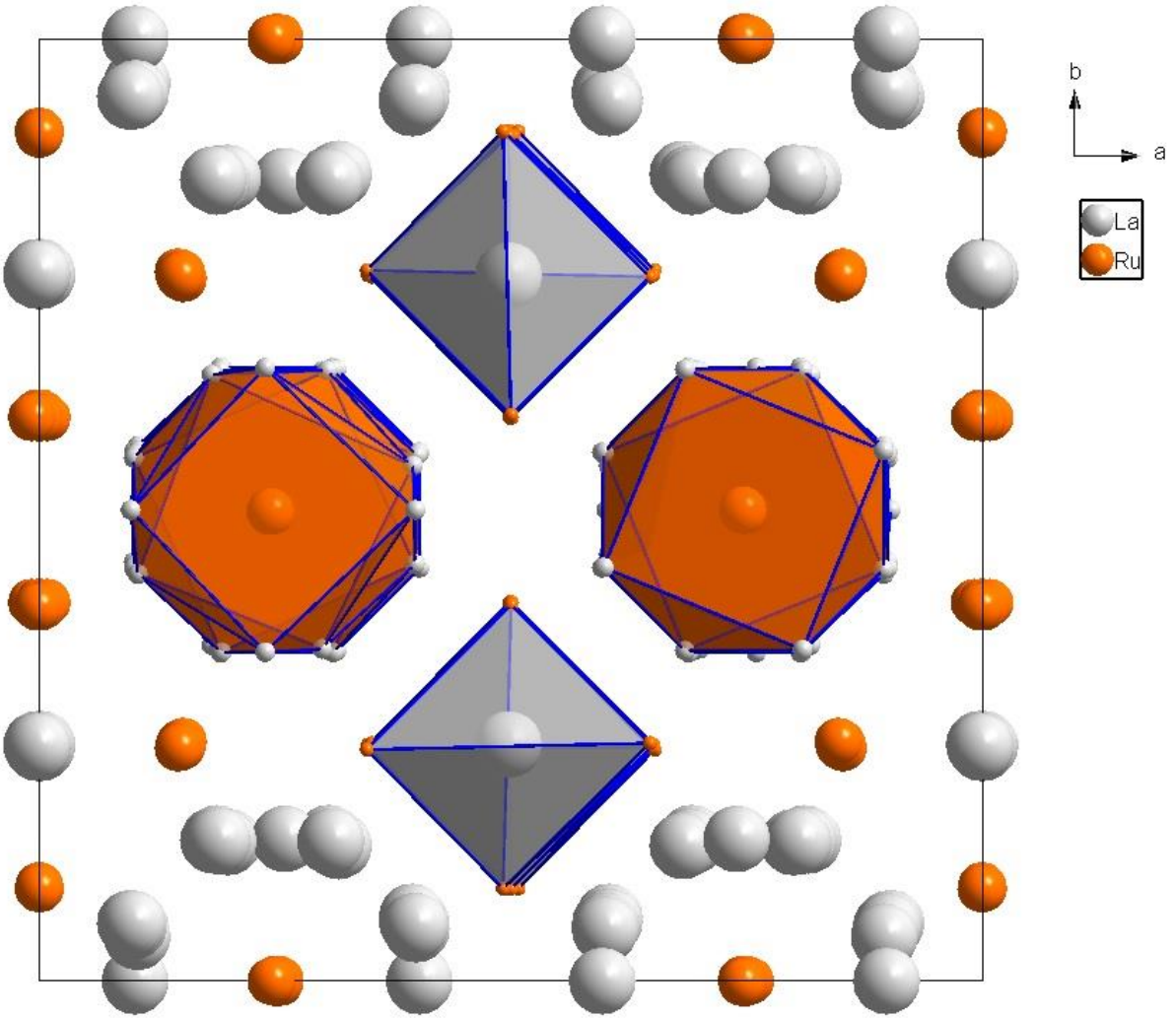

Figure 11. A cut out section of the *C222₁* structure showing how the square antiprism and tetrahedron form their respective columns along the c-direction.

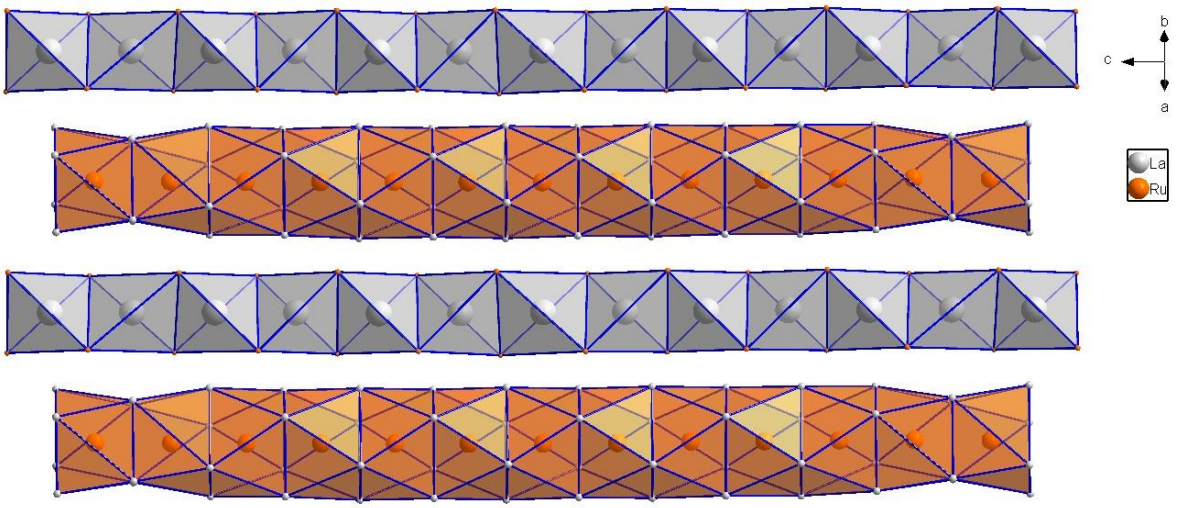

The tetragonal solution was refined using the *P422* space group and the cell parameters a = 16.0154(4) (Å), b = 16.0154(4) (Å), c = 35.5547(9) (Å). The refinement ended with R_{obs} = 12.55 % over 6770 observed reflections. The structure is described with 58 atomic positions, these positions can be found in appendix B along with complete list of crystallographic and technical data for the structure refinement.

As in the orthorhombic solution some ruthenium atoms are surrounded by eight lanthanum atoms in the form of square antiprism which forms columns of face sharing antiprisms along the c-direction. Because of the tetragonal lattice the square anti prism columns now translate at the centre of the ab plane of the unit cell. The rest of the ruthenium atoms are surrounded by four lanthanum atoms in the form of tetrahedron which share edges along the c-direction and form columns that surround the square anti prism columns (Figure 12, 13).

Figure 12. The unit cell of the *P422* structure solution of $LaRu_x$ observed along the c-direction with tetrahedrons and square antiprism.

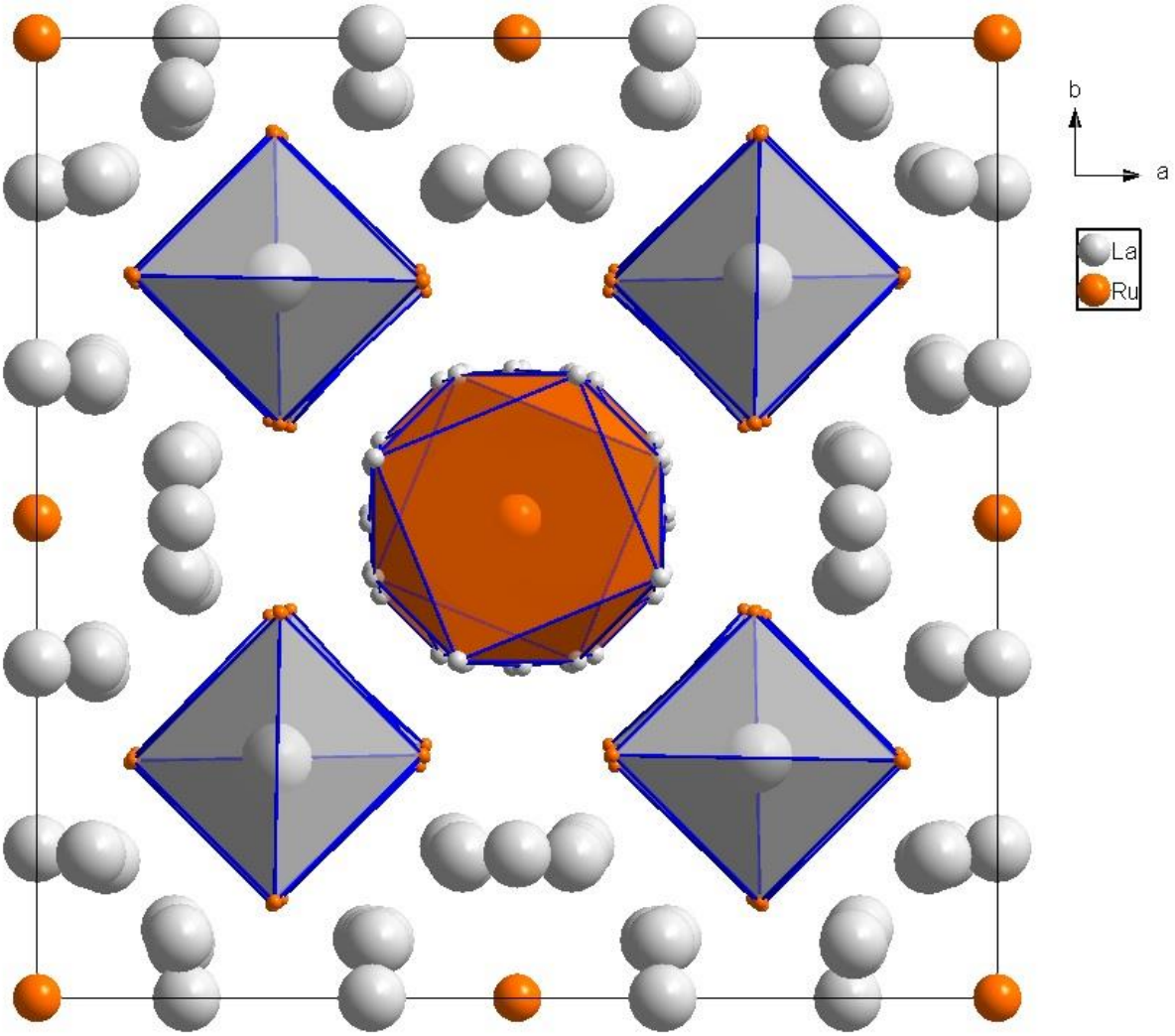

Figure 13. A cut out section of the *P422* structure showing how the square antiprism and tetrahedron form their respective columns along the c-direction.

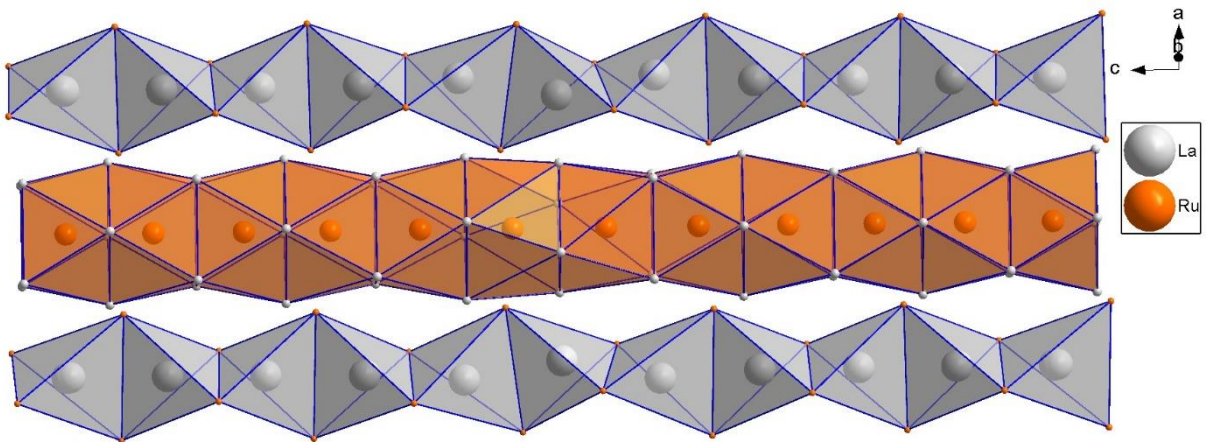

In the $Y_{44}Ru_{25}$ case we saw that the orthorhombic and the tetragonal lattices were symmetry incompatible. For the *P422* and the *C222₁* solutions this is not the case. The tetragonal solution contains orthogonal operations and can readily transform into an orthogonal sub cell. Therefore we cannot, as in the $Y_{44}Ru_{25}$ case, draw any conclusions about the superspace solution from the best $LaRu_x$ solutions. However, the presence of satellite reflections and the fact that the reflection positions to not completely agree with the three-dimensional solution strongly suggest that the structure is aperiodic and can be better described in higher dimensions.

Because of the similarity's in diffraction pattern and stoichiometry between the $Y_{44}Ru_{25}$ and $LaRu_x$ there is reason to believe that the two phases should be regarded as one singular phase. Then the space group of the higher-dimensional for the structures would be the same and we should be able to solve the the $LaRu_x$ phase with the two three-dimensional solutions *Pnna* and *P4/n*. The results from this investigation was however inconclusive. The *P4/n* solution was possible but subpar to that of the previously mentioned solutions and the *Pnna* could not be solved. That this was not possible can however be attributed to the rather messy diffraction patterns and better diffraction patterns might give the theorized results.

The higher-dimensional description would prove this theory but has proven to be difficult and time consuming and will not be performed in this thesis.

5. Conclusion and Future Work

The structure of the incommensurately modulated two composite compound Er_3Ru_2 has been solved. The first subsystem comprises of Ru1 at (2/3, 0, 2.44696), Ru2 at (-2/3, 0 – 0.244696), Y1 at (0.559234, -0.173222, -0.245914) and Y2 at (-0.559234, 0.173222, 0.245914) and the second subsystem is built up exclusively of Ru3 atoms in position (0, 0, 0). The structure was solved using the current (3+1)d superspace approach from structure data which was collected with x-ray single-crystal diffraction. The structure solution, performed with the charge-flipping algorithm, resulted in the non-centrosymmetric super-space group *X3 (00γ)0* with $a = b =$ 13.893 (4) Å, c = 4.0005 (12) Å q = 1.572 c*.

The possibility for superstructure descriptions for the $Y_{44}Ru_{25}$ and the $LaRu_x$ compounds were also investigated. The diffraction patterns of both compounds contained satellite reflections, indicating superstructure. Additionally the $Y_{44}Ru_{25}$ structure could be solved well with two symmetry incompatible lattices further strengthening the possibility of superstructure. It was hypothesised that the two phases are the same but this was not conclusively proven in this report. It could be concluded that these compounds most likely can be well described with the superspace description, however the task of describing them in higher-dimensions was not completed in this thesis and is considered future work.

An important aspect to consider is the ethical foundation of a project like this. There is at the moment no direct application of the results concluded in this report but scientific discoveries rarely happen overnight. It's essential to always strive towards increasing the scientific knowledge, who knows what discoveries results such as this might inspire or lead to in the future.

6. References

[1] C. J. Raub, *Handbook on the physics and chemistry of rare earths, volume 21*, vol. 255. 1997.

[2] E. Tominez, E. Tominez, E. Alleno, E. Alleno, P. Berger, P. Berger, M. Bohn, M. Bohn, C. Mazumdar, C. Mazumdar, C. Godart, and C. Godart, "Chemical and Superconducting Properties of the Quaternary Borocarbides Ln-M-B-C (Ln=rare earths, Y; M=Ni, Pd)," *J. Solid State Chem.*, vol. 154, pp. 114–129, 2000.

[3] R. Kumar, C. V. Tomy, R. Nagarajan, P. L. Paulose, and S. K. Malik, "Magnetization and heat capacity studies of double perovskite compounds Ba2SmRuO6 and Ba2DyRuO6," *Phys. B Condens. Matter*, vol. 404, no. 16, pp. 2369–2373, 2009.

[4] a. Palenzona and F. Canepa, "New compounds in the 30–40 at.% Ru range of the rare earth-ruthenium (R-Ru) systems," *J. Less Common Met.*, vol. 162, pp. 267–272, 1990.

[5] M. . Fornasini, A. Mugnoli, and A. Palenzona, "Crystal structure of Y44Ru25," *Journal of the Less Common Metals*, vol. 154, no. 1. pp. 149–156, 1989.

[6] A. Palenzona and F. Canepa, "THE PHASE DIAGRAMS OF THE La-Ru AND Nd-Ru SYSTEMS," vol. 157, pp. 307–313, 1990.

[7] J. Sun, S. Lee, and J. Lin, "Four-dimensional space groups for pedestrians: Composite structures," *Chem. - An Asian J.*, vol. 2, no. 10, pp. 1204–1229, 2007.

[8] M. L. Fornasini and A. Palenzona, "The crystal structure of Er 3 Ru 2," *Zeitschrift für Krist.*, vol. 192, no. 3–4, pp. 249–254, 1990.

[9] M. L. Fornasini and a. Palenzona, "Sr7Pt3: An orthorhombic structure formed by Pt-centered trigonal prisms," *J. Solid State Chem.*, vol. 47, no. 1, pp. 30–33, 1983.

[10] B. Davaasuren, "Intermediate phases in the ternary systems RE - T -C (RE = Y , La , Gd-Er ; T = Cr , Fe , Ru)," University of Technology, Dresden, 2010.

[11] P. Sharifrazi, A. Raman, and R. C. Mohanty, "Intermediate phases in some rare earth-ruthenium systems," vol. 16, no. Zeitschrift fuer Metalkunde, pp. 801–805, 1984.

[12] B. Hillenbrand and M. Wilhelm, "Superconductivity in rare earth-ruthenium laves phases," *Physics Letters A*, vol. 33, no. 2. pp. 61–62, 1970.

[13] L. E. Smart and E. A. Moore, *Solid State Chemistry: An Introduction*, Fourth Edi. Boca Raton: CRC Press Taylor & Francis Group, 2012.

[14] C. Giacovazzo, H. L. Monaco, D. Viterbo, F. Scordari, G. . Gilli, G. Zanotti, and M. Catti, *Fundamentals of Crystallography*. Oxford: Oxford University Press, 1992.

[15] L. Palatinus and G. Chapuis, "SUPERFLIP - A computer program for the solution of crystal structures by charge flipping in arbitrary dimensions," *J. Appl. Crystallogr.*, vol. 40, no. 4, pp. 786–790, 2007.

[16] G. Oszlányi and A. Süto, "The Charge Flipping Algorithm," *Acta Crystallogr.*, pp. 123–134, 2008.

[17] S. Van Smaalen, "An elementary introduction to superspace crystallography," *Zeitschrift fur Krist.*, vol. 219, no. 11, pp. 681–691, 2004.

[18] a. Yamamoto, "Crystallography of Quasiperiodic Crystals," *Acta Crystallogr. Sect. A Found. Crystallogr.*, vol. 52, no. 4, pp. 509–560, 1996.

[19] V. Petříček and M. Dušek, "Methods of structural analysis and computer program JANA2000," *Zeitschrift für Krist.*, vol. 219, no. 11–2004, pp. 692–700, 2004.

[20] H. T. Stokes, B. J. Campbell, and S. Van Smaalen, "Generation of (3 + d)-dimensional superspace groups for describing the symmetry of modulated crystalline structures," *Acta Crystallogr. Sect. A Found. Crystallogr.*, vol. 67, no. 1, pp. 45–55, 2011.

[21] a. Yamamoto, "Determination of composite crystal structures and superspace groups," *Acta Crystallogr. Sect. A Found. Crystallogr.*, vol. 49, no. 6, pp. 831–846, 1993.

[22] V. Petříček, M. Dušek, and L. Palatinus, "Crystallographic Computing System JANA2006: General features," *Zeitschrift für Krist. ...*, vol. 229, no. 5, pp. 345–352, 2014.

[23] L. Palatinus, "Ab initio determination of incommensurately modulated structures by charge flipping in superspace," *Acta Crystallogr. Sect. A Found. Crystallogr.*, vol. 60, no. 6, pp. 604–610, 2004.

[24] "WinXPow." Stoe & Cie, Darmstadt, Germany, 2011.

[25] "CrysAlisPRO." Oxford Diffraction /Agilent Technologies UK Ltd, Yarnton, England, 2012.

[26] Dr. H. Putz and D. K. Brandenburg, "Diamond - Crystal and Molecular Structure Visualization." Kreuzherrenstr. 102, 53227 Bonn, Germany.

Appendix A

Table A1. List of all synthesis prepared. Diffraction data from crystals obtained from samples in bold were used for structure evaluation.

Sample	Estimated at.% Ru	Annealing T (K)	Annealing t (Days)
$Y_{44}Ru_{25}$ 1.0	**38**	**770**	**12**
$Y_{44}Ru_{25}$ 2.0	36	770	12
$Y_{44}Ru_{25}$ 3.1	39	800	10
$Y_{44}Ru_{25}$ 3.1	40	800	10
$Y_{44}Ru_{25}$ 4.1	34	800	10
$Y_{44}Ru_{25}$ 4.2	33	800	10
$Y_{44}Ru_{25}$ 4.3	35	800	10
$LaRu_x$ 1.0	36	770	12
$LaRu_x$ 2.0	34	770	12
$LaRu_x$ 3.1	38	770	10
$LaRu_x$ 3.2	37	770	10
$LaRu_x$ 3.3	**39**	**770**	**10**
Er_3Ru_2 1.0	40	770	12
Er_3Ru_2 2.1	42	1100	10
Er_3Ru_2 2.2	43	1100	10
Er_3Ru_2 2.3	44	1100	10

Appendix B

Table B1. Crystallographic and technical data.

Empirical formula	Y3Ru2	$LaRu_x$	$Y_{44}Ru_{25}$
M [g mol^{-1}]	469	-	6438
Crystal system	Rhombohedral	Orthorhombic/Tetragonal	Orthorhombic/Tetragonal
Space group	X3(00γ)0	$C222_1$/P422	Pnna/P4/n
a [Å]	13.895	16.0157	15.2584
b [Å]	13.895	16.0157	15.2584
c [Å]	4.0001	35.5547	28.033
Modulation wave vector	1.572 c*	-	-
Diffractometer	Oxford Diffraction XCaliburE	Oxford Diffraction XCaliburE	Oxford Diffraction XCaliburE
Radiation, λ [Å]	Mo $K\alpha_1$ λ = 0.7107	Mo $K\alpha_1$ λ = 0.7107	Mo $K\alpha_1$ λ = 0.7107
T [K]	RT	RT	RT
Reflections measured	726	11226	7279
Observed reflections ($I > 3\sigma$)	625	6770	1426
Data reduction	CrysAlisPro	CrysAlisPro	CrysAlisPro
Absorption correction	-	-	-
Structure solution, refinement	Jana2006, Superflip	Jana2006, Superflip	Jana2006, Superflip
R_{obs} main	2.86 %	11.77/12.55 %	14.73/8.49 %
R_{obs} composite 1	2.68 %	-	-
R_{obs} composite 2	4.64 %	-	-
R_{obs} common	2.51 %	-	-

Table B2. Atom position for the Er_3Ru_2 *X3(00γ)0* structure solution.

Atom	x	y	z	Atom	x	y	z
Ru1	0.666667	0.000000	0.244696	Y1	0.559234	-0.173222	-0.245914
Ru2	-0.666667	0.000000	-0.244696	Y2	-0.559234	0.173222	0.245914
Ru3	0.000000	0.000000	0.000000				

Table B3. Atom position for the $Y_{44}Ru_{25}$ *P4/n* structure solution.

Atom	x	y	z	Atom	x	y	z
Ru1	0.240459	0.102673	0.367983	Y2	0.157132	0.514558	0.443219
Ru2	0.500000	0.000000	0.166515	Y3	0.444646	0.149645	0.334684
Ru3	0.500000	0.000000	0.277409	Y4	0.355576	0.073393	0.444107
Ru4	0.000000	0.500000	0.052682	Y5	-0.064301	0.348767	0.216369
Ru5	0.000000	0.000000	0.444702	Y6	0.060532	0.142006	0.387660
Ru6	0.500000	0.000000	0.499774	Y7	0.251328	0.749043	0.187934
Ru7	0.000000	0.500000	0.268937	Y8	0.248423	0.251976	0.312880
Ru8	0.250572	-0.098000	0.484567	Y9	0.146514	0.067010	0.498649
Ru9	0.500000	0.000000	0.391116	Y10	0.150106	0.057275	0.280856
Ru10	0.000000	0.000000	0.000000	Y11	0.145888	0.436870	-0.002216
Ru11	0.000000	0.000000	0.226551	Y12	0.352897	0.557779	0.169077
Ru12	0.401201	0.247889	0.252015	Y13	-0.057941	0.149130	0.282412
Ru13	0.000000	0.500000	0.384832	Y14	0.063555	0.349255	0.107884
Ru14	0.251516	0.599600	0.246949	Y15	0.649161	0.064835	0.111654
Ru15	0.500000	0.500000	0.114094	Y16	0.352798	0.062678	0.221778

Ru16	0.000000	0.000000	0.335759	Y17	0.155606	-0.067641	0.393817
Ru17	0.099000	0.756773	0.129123	Y18	0.148440	0.557490	0.325612
Ru18	0.000000	0.500000	0.161055	Y19	0.442702	0.352442	0.171811
Ru19	0.000000	0.500000	-0.057955	Y20	0.245830	0.750494	0.062711
Ru20	0.402587	0.743635	0.129856	Y21	0.344698	0.508089	0.056025
Ru21	0.230233	0.407495	0.372538	Y22	0.341482	0.502321	-0.058573
Ru22	0.248353	0.599807	0.014836	Y23	0.363348	0.425700	-0.056963
Ru23	0.249528	0.597266	-0.016578	Y24	0.356770	0.428688	0.055958
Y1	0.245830	0.750494	0.062711				

Table B4. Atom position for the $LaRu_x$ *P422* structure solution.

Atom	x	y	z	Atom	x	y	z
La1	0.231341	0.231341	0.500000	La30	0.500000	0.150078	0.000000
La2	0.155746	0.000000	0.500000	Ru1	0.500000	0.500000	0.268840
La3	0.558257	0.148505	0.184544	Ru2	0.500000	0.000000	0.500000
La4	0.945167	0.149440	0.314072	Ru3	0.500000	0.500000	0.089138
La5	0.851204	0.062641	0.222385	Ru4	0.000000	0.000000	0.088926
La6	0.735354	0.738040	0.400637	Ru5	1.000000	0.000000	0.180581
La7	0.747188	0.251528	0.299903	Ru6	0.245105	0.096752	0.442975
La8	0.439368	0.148933	0.274935	Ru7	0.500000	0.000000	0.319923
La9	0.856570	0.071894	0.405286	Ru8	0.900003	0.250095	0.250818
La10	0.556921	0.145374	0.365425	Ru9	0.745591	0.103330	0.346013
La11	0.852742	0.062041	0.043861	Ru10	0.597247	0.251836	0.247967
La12	0.150037	0.057313	0.132604	Ru11	0.000000	0.000000	0.359072

La13	0.438507	0.350979	0.222291	Ru12	0.500000	0.500000	0.000000
La14	0.749060	0.249955	0.199696	Ru13	0.500000	0.000000	0.046645
La15	0.343301	0.061600	0.368115	Ru14	0.500000	0.000000	0.227662
La16	0.651193	0.058848	0.275393	Ru15	0.500000	0.000000	0.137366
La17	0.557993	0.348865	0.132291	Ru16	1.000000	0.000000	0.268254
La18	0.433919	0.157533	0.457511	Ru17	0.500000	0.500000	0.456023
La19	0.184715	0.057632	0.184715	Ru18	0.500000	0.500000	0.361968
La20	0.437522	0.350924	0.044022	Ru19	0.150776	0.400007	0.150776
La21	0.642577	0.060113	0.453654	Ru20	0.753211	0.101919	0.153671
La22	0.553500	0.349908	0.314618	Ru21	0.736394	0.404044	0.348439
La23	0.750966	0.250418	0.100269	Ru22	0.757931	0.602070	0.459994
La24	0.854402	0.442102	0.092883	Ru23	0.598825	0.252841	0.053269
La25	0.642109	0.580230	0.500010	Ru24	0.500000	0.500000	0.180939
La26	0.646582	0.057580	0.093067	Ru25	0.000000	0.000000	0.452532
La27	0.348587	0.000000	0.000000	Ru26	1.000000	0.000000	0.000000
La28	0.748872	0.248581	-0.001172	Ru27	0.500000	0.000000	0.408093
La29	0.654100	0.495425	0.409643	Ru28	0.899884	0.247194	0.056131

Table B5. Atom position for the $LaRu_x$ *C222₁* structure solution.

Atom	x	y	z	Atom	x	y	z
La1	0.498987	0.252517	0.199941	La24	0.604449	0.068045	0.093765
La2	0.599834	0.442083	0.222656	La25	0.739575	0.150928	0.000743
La3	0.188291	0.151368	0.222970	La26	0.596988	0.000000	0.000000
La4	0.101897	0.057698	0.314547	La27	0.898510	0.000000	0.000000
La5	0.399557	0.061755	0.224140	La28	-0.199948	0.147481	0.094550
La6	0.304896	0.352088	0.184826	Ru1	0.000000	0.099979	0.250000

La7	0.689075	0.351063	0.133583	Ru2	0.500000	-0.097823	0.250000
La8	0.184643	0.149308	0.044303	Ru3	0.745881	0.500000	0.000000
La9	0.808795	0.352162	0.223242	Ru4	0.251043	0.001424	0.270460
La10	0.898475	0.441536	0.133457	Ru5	0.348595	0.250622	0.248477
La11	0.395390	0.063032	0.044525	Ru6	0.747356	0.500421	0.090677
La12	-0.002218	0.251492	0.199568	Ru7	0.750894	0.501848	0.180539
La13	0.307928	0.151592	0.133112	Ru8	0.745029	0.001534	0.046520
La14	0.598671	0.439003	0.043287	Ru9	-0.150526	0.253462	0.152136
La15	0.307002	0.151213	0.315611	Ru10	0.253465	0.001705	0.361415
La16	0.400008	-0.055019	0.315681	Ru11	0.497743	0.102923	0.152751
La17	-0.002077	0.248522	-0.100936	Ru12	0.148693	0.252016	0.152690
La18	0.809612	0.351702	0.044230	Ru13	0.498932	0.401929	0.152456
La19	0.596554	0.561202	0.133236	Ru14	-0.008142	0.401810	0.050974
La20	-0.003133	0.250733	0.100176	Ru15	0.147452	0.247460	-0.055375
La21	0.396052	0.453103	0.093147	Ru16	-0.152593	0.254409	-0.051751
La22	-0.002332	0.248965	-0.000716	Ru17	0.000353	0.101070	0.056292
La23	0.182524	0.356621	0.093371				